

CRUDE OIL FOULING MITIGATION USING INTERNALLY FINNED TUBES

H.M. Joshi¹, T. Lang², J. El Hajal², and A.D. Smith³

¹ Shell Global Solutions (US) Inc., 3333 Highway 6 South, Houston TX 77082 USA; himanshu.joshi@shell.com

² Wieland-Werke AG, Graf-Arco-Str. 36, 89079 Ulm, Germany

³ Heat Transfer Research, Inc., P. O. Box 1390, Navasota, TX 77868 USA

ABSTRACT

Fouling of crude oils inside heat exchanger tubes is strongly dependent on wall shear stress – with higher shear stresses leading to decreasing rates of fouling. In this paper we show that tube side heat transfer enhancement techniques which depend on increased wall shear stress, or create an effect similar to increased wall shear stress, also reduce fouling in a typical crude oil fouling situation.

Heat transfer and fouling data was taken on a double pipe heat exchanger with the crude and hot side fluids both at the highest temperature values encountered in an oil refinery.

At the same nominal velocity (i.e., based on a plain ID for both tubes), the tests showed a 57% fouling reduction using the Wieland Low Fouling (LF) inside structure tube, with the fouling resistance calculated on the basis of the plain outer surface area, which is equal for both tubes. The clean pressure drop and heat duty also showed increases due to the structured tube. Such data can be used to predict the effect of similar mitigation techniques and to economically justify the use of these techniques in operating facilities.

INTRODUCTION

Viscous shear stress at the tube wall is known to be a critical factor in crude oil fouling. Heat transfer enhancement techniques which depend on changing the flow pattern near the tube wall result in increased shear stress, and might provide the added benefit of fouling mitigation. The price paid is in higher pressure drop compared to an unenhanced tube.

One such enhancement technique is internal fins, typically arranged in a helical pattern along the tube length. This paper presents heat transfer, pressure drop, and fouling rate data for the Wieland Low Fouling (LF) inside structure; and compares the results to an unenhanced (plain) tube. A sketch of a typical internal finned tube is shown in Fig. 1.

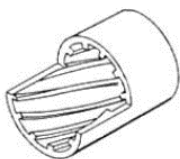


Fig. 1 Typical Internal Finned Tube.

Data was collected in a pilot-plant scale fouling test unit located at the Shell Bangalore Laboratories in India. The test section was a double pipe heat exchanger, with the Wieland LF tube as the inner tube with crude oil flow. Heating was provided by a hot oil entering the shell side, in a counterflow arrangement. A photo of the double pipe test section is shown in Fig. 2, where the nozzle at the right is the shell side inlet (into the annulus of the double pipe), and the crude outlet is at the bottom right (out from the inner tube). Both the crude and the hot oil recirculate in the test unit. Heat is provided to the hot oil using electrical heaters and removed from the crude using an aircooled heat exchanger.



Fig. 2 Photo of Fouling Test Section.

Test measurements used to calculate heat transfer and fouling are inlet and outlet temperatures and flow rates on each side. The tests are run with fixed inlet temperatures for the crude and the hot oil, with the crude flow set to achieve a desired velocity. Hot oil flow is set at a very high velocity (>3 m/s) to ensure that the impacts of crude flow and fouling are dominant. Most tests show a fouling induction period where the heat duty increases, before the trend reverses and fouling is presumed to begin.

The enhanced tube was tested at one flow rate (velocity) and the resulting fouling rate was compared to a baseline fouling rate curve for plain tubes, generated at five velocities.

TEST RESULTS

Starting from the point where induction ends, fouling resistance (R_f) is calculated on an hourly basis (using minute average data for the previous hour) and plotted as a function of time. The slope of the R_f curve is the fouling rate expressed in the units of [m²-C/W/day]

R_f is calculated as follows:

$$Q = m C_p (T_{c_o} - T_{c_i}) \quad (1)$$

$$U = Q/A/LMTD \quad (2)$$

$$R_f = 1/U_f - 1/U_0 \quad (3)$$

The specific heat (C_p), density, and viscosity of the crude were calculated using crude assay information input into a process simulator. Flows, temperatures, and all other quantities are directly measured or calculated using measured values. The uncertainties in measurements were as follows, based on instrument calibration and calculated uncertainties: temperature - $\pm 0.1^\circ\text{C}$; mass flow rate - $\pm 0.1\%$; calculated fouling resistance - $\pm 3.0\%$. The fouling resistance uncertainty was obtained by using software which calculates the uncertainty of a calculated quantity using the uncertainty of each component.

The starting steady state conditions (i.e., the clean conditions) for the enhanced tube test are listed in Table 1, and Table 2 shows the geometry of the two tubes. The material of construction was carbon steel (mild steel) in both cases.

Table 1. Starting Steady-State Conditions.

Crude inlet temperature, $^\circ\text{C}$	241.8
Crude outlet temperature, $^\circ\text{C}$	274.1
Hot oil inlet temperature, $^\circ\text{C}$	339.6
Hot oil outlet temperature, $^\circ\text{C}$	332.1
Heat duty, kW	24.9
Tube side velocity, m/s	1.2
Tube shear stress, plain, Pa	2.9
Tube shear stress, enhanced, Pa	5.5

The tube side velocity in Table 1 is a nominal velocity, calculated using an ID of 21.4 mm. That is, it does not account for the cross-sectional area of the LF structure. The shear stress in the last row was calculated using Wieland's proprietary friction factor correlation for the internal fin.

Table 2. Tube geometries.

	Plain tube	LF tube
Outside diameter, mm	25.40	25.40
Wall thickness, mm	2.77	2.00
Inside diameter (plain portion for LF), mm	19.86	21.40
Length, m	3.0	3.0
Area enhancement ratio relative to plain tube	1.0	1.3

Fig. 3 shows the fouling resistance trend for the enhanced tube over a period of 28 days, which includes an induction period of about 16 days. For this figure we used the pre-induction steady state as the zero-fouling point (to set U_0). Fig. 4 shows the development of fouling resistance over time for the two tubes, using the end of induction as the zero-fouling point.

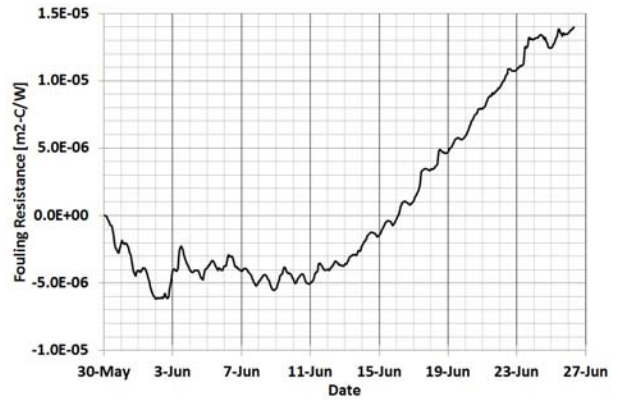


Fig. 3 Steady state fouling resistance trend for the LF enhanced tube.

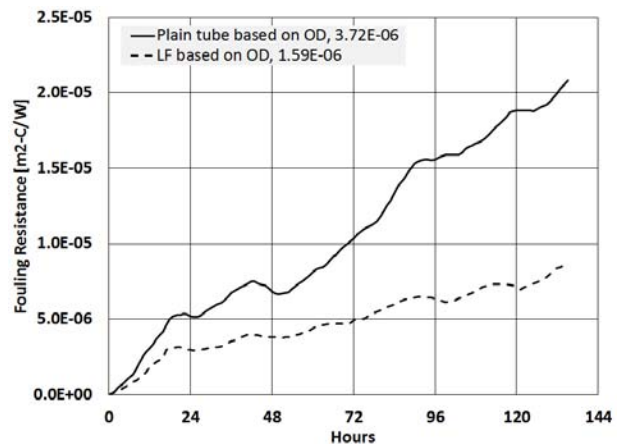


Fig. 4 Post induction fouling resistance trend for enhanced and plain tube. Fouling rates in units of $\text{m}^2\text{-C/W/day}$ are shown in the legend.

Fig. 5 shows the fouling rate comparison between the baseline plain tube and the enhanced tube. The plain tube curve was generated from data at five velocities, and the rate on the Y-axis represents the slopes of curves similar to Fig. 4. The plain tube curve is a power-law fit of the five data points with an R^2 value = 0.94. The velocity on the X-axis is the nominal velocity as noted earlier. The fouling rate of the enhanced tube is 43% that of the plain tube at the same nominal velocity. Put another way, the enhanced tube provides the same fouling resistance as a plain tube would at a velocity of 1.7 m/s, or it will take 2.3 times the duration for the same amount of fouling to accumulate in the enhanced tube, assuming linear rates.

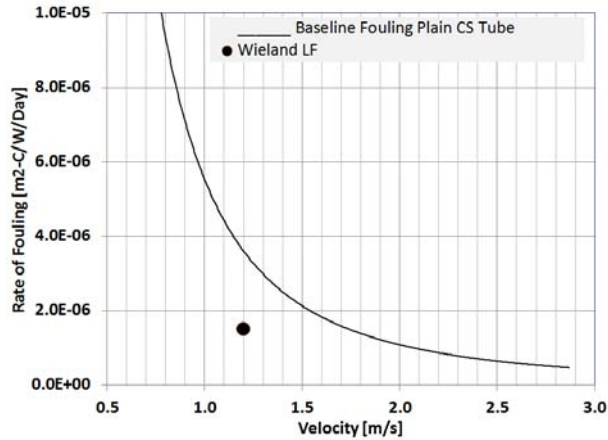


Fig. 5 Comparison of fouling rates - plain vs enhanced tube.

The values in Figs. 3-5 are based on the tube external surface (25.4mm dia.). If based on the internal surface (plain or enhanced) the relative fouling rate values are different, as will be discussed later in this paper.

Based on the external surface, the relative heat transfer and pressure drop performances of the two types of tubes are shown in Table 3. As expected, the heat transfer is enhanced but at the price of increased pressure drop.

Table 3. Comparison of Performance.

	Plain	Enhanced (LF)	Ratio - Enh/Plain
Clean Heat Duty, kW	20.5	24.9	1.21
Clean Pressure Drop, kPa	1.47	2.40	1.63
Clean overall heat transfer coefficient, W/m ² -C	1109.1	1360.4	1.23
Fouling Rate, m ² -C/W/day	3.72E-06	1.59E-06	0.43

DISCUSSION

We will discuss a few important points based on the above data.

Comparing the fouling performance of different tube geometries

The two tube varieties we tested have the same OD (25.4 mm) but different wall thicknesses, resulting in different plain surface IDs. The plain tube is 2.77 mm thick with an ID of 19.86 mm, while the LF tube is 2 mm thick with an ID of 21.4 mm. In addition, the LF tube has a fin structure which increases the inside surface by 27%.

Since the fouling is on the inside of the tube, using internal surface area may provide a fairer comparison, see

Table 4. Based on the OD the LF tube fouls at a rate of 43% relative to the plain tube (row 1).

However, if the comparison is based on the inside surface area corresponding to a 2mm wall thickness (row 2) the relative fouling is slightly higher at 46%, and if we take into account the extra surface area provided by the internal structure (row 3) the relative fouling is 55%. When evaluating a heat exchanger with LF tubes, it would be appropriate to use the 55% value, which corresponds to a decrease of 45% in fouling rate.

Table 4. Fouling rate comparison based on different surface areas.

Comparison basis	LF fouling rate as % of plain tube fouling rate
OD to OD, 25.4mm for both	43%
(OD-4mm), i.e., based on 21.7 mm ID for both	46%
Enhanced surface for LF vs. 19.86mm ID for plain	55%

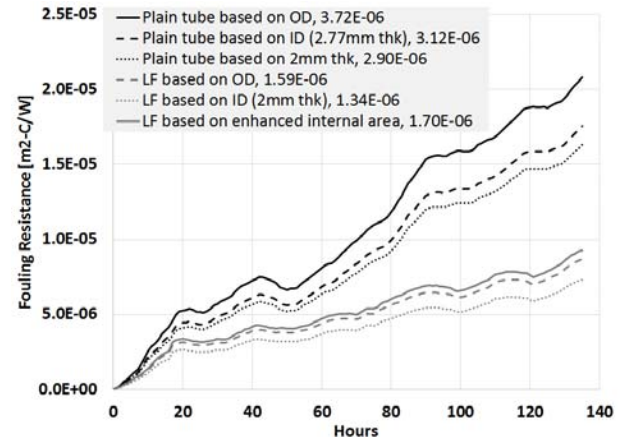


Fig. 6 Measured fouling resistance based on different surface areas for the plain and LF tubes. Fouling rates (the slope of each line) are shown in the legend in the units of [m²-C/W/day].

Fig. 6 shows the fouling curves based on the area comparisons in Table 4. The ratios of the slopes from Fig. 6 produce the percentages shown in Table 4.

Use of the LF technology to improve design and operation of crude heat exchangers

When trying to mitigate fouling in an existing heat exchanger, or when designing a new heat exchanger, the heat transfer and fouling benefits of an enhanced tube can be used to offset the cost of extra pressure drop and the marginal incremental cost of the tubes. One method to perform such an evaluation of benefits is PEC -- Performance Evaluation Criteria, (Joshi et. al. 2014). There

it was shown, for a similar enhancement technique, that the benefits can be in terms of increased heat duty with the same heat exchanger size (but increased pressure drop), or smaller flow rates of the heat source to achieve the same heat duty, while retaining the heat exchanger size.

For the LF tube we performed simple case studies on one shell-and-tube heat exchanger service having 2 shells in series, with 536 carbon steel tubes of 19.05mm OD and 6m length. Field performance shows that this heat exchanger reaches a fouling resistance value of 0.0097 m²-C/W in one year of operation.

Corresponding to the above fouling rate, the heat duty during operation decreases from a clean value of 4.8 MW to 1.7 MW in one year. If the tube bundles were to be replaced with LF tubes, the corresponding heat duties are 5.1 and 2.4 MW, using a fouling resistance of 0.0058 m²-C/W, corresponding to a 45% improvement (row 3, Table 4). The improvement provided by the LF tubes results in an average heat duty increase of 0.5 MW over a one-year period. The pressure drop increase in the clean condition is 11 kPa (from 20 to 31 kPa) which needs to be justified based on the increase in heat duty.

Two other ways to evaluate the improvement are to estimate the increase in run length with the LF tubes before it reaches the same level of fouling as the plain tubes; or to consider a smaller heat exchanger which can give the same performance. The run length increase is 82% which is simply the ratio of the fouling rates (inverse of the reduction in row 3, Table 4). This benefit comes with the same 11 kPa pressure drop increase. If a redesign was feasible, a shorter tube length of 4.4m will provide the same performance, including pressure drop to match the plain tubes.

Comparison of data and theoretical calculations

Heat transfer coefficient and pressure drop calculations for the double pipe geometry used in our tests are well established. For the LF tube, Wieland has developed calculation methods based on internal testing. We compared measured versus calculated values of heat transfer coefficient and pressure drop for both tubes, and found differences up to 38%. Table 5 summarizes the comparisons.

Table 5. Data vs calculations.

Tube Type	Plain	Ratio to meas.	LF	Ratio to meas.
Measured Data				
Overall heat transfer coefficient, W/m ² -C	1096	--	1342	--
Tubeside pressure drop, kPa	1.49	--	2.41	--
Calculated Values				
Overall heat transfer coefficient, W/m ² -C	683	0.62	1173	0.87
Tubeside pressure drop, kPa	1.86	1.25	3.05	1.27

The most likely cause of the heat transfer coefficient discrepancy is the presence of dissolved nitrogen in the crude, which bubbles when heated in the test heat exchanger and enhances heat transfer. This phenomenon has been described by Fetisoff et.al. (1982), Hout (1983), and Harris et. al. (2017). The fouling tests were conducted with the crude side pressure maintained at 45 barg using a nitrogen blanket which accounts for the dissolved nitrogen. Heat Transfer Research Inc. (HTRI) has now discontinued the practice of using nitrogen for pressurization based on the findings described in Harris et. al. (2017).

The pressure drop discrepancy is likely due to the design and location of the pressure taps which over many tests have given similar differences with calculations.

Impact of shear stress

The effect of tubeside enhancement on fouling can be thought of as an increase in shear stress. The shear stress for the plain tube conditions was 2.9 Pa, and Fig. 6 shows that the enhanced tube acts like a plain tube with a shear stress of about 5.5 Pa, close to the calculated value shown in Table 1. Thus, if the shear stress for an enhancement technique such as the LF structure can be calculated, it may be possible to predict the fouling rate with the enhancement, using a baseline curve such as the one in Fig. 7.

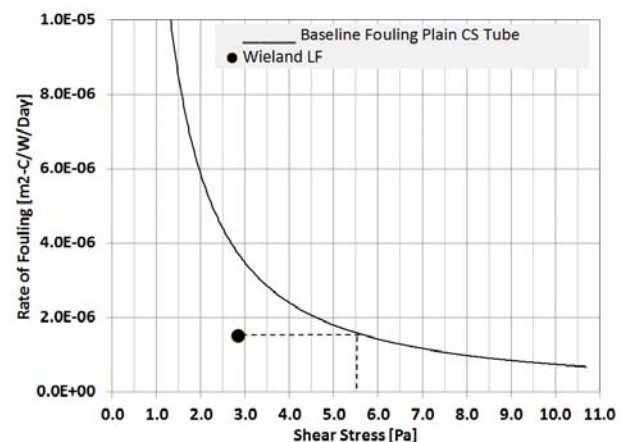


Fig. 7 Comparison of fouling rates - plain vs enhanced tube, based on tube side shear stress.

The average shear stress in an LF tube could possibly be calculated using accurate pressure drop measurements, but it may not be sufficient to correlate to fouling because of the non-uniform nature of the internal structure.

Webb and Li (2000) showed that the fouling in enhanced tubes is strongly dependent on the structure itself. So the velocity or pressure drop with enhanced tubes do not give sufficient information about the local effective wall shear stress. Webb (2005) showed a relationship between fouling and the number of “ridges” and fin pitch for a tube similar to the LF tube.

Two different situations are schematically represented in Fig. 8. In the top sketch, with a small fin spacing, the main fluid flow goes over the fins and there is recirculation between the fins. In contrast the bottom sketch shows a

wide fin spacing where main fluid flow impacts the front of the fin. The local wall shear stress in the flow recirculation zones could even be lower than the one for a smooth tube with the same mean fluid velocity and is therefore favorable for fouling development. The wall shear stress is higher at the top of the fins and front side of the fins where the fluid impacts and is higher than for a smooth tube with the same mean velocity.

The non-uniformity of shear stress and consequently of the fouling formation provides for a large uncertainty in the ability to predict the correct shear stress in the LF structure to correlate to fouling. Further, it can be assumed that the high shear stress on both the top and front of the fins can explain the increase in heat transfer and reduction of fouling rate.

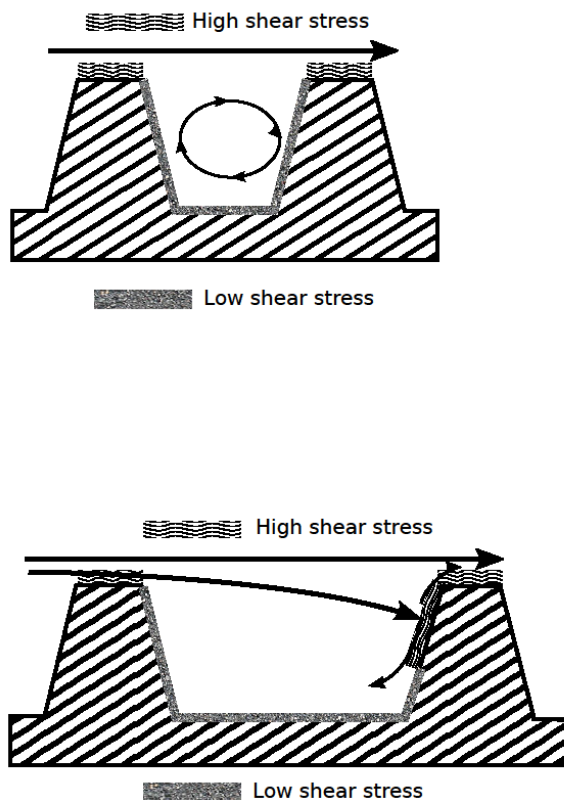


Fig. 8 Flow patterns over different internal structure geometries.

Uncertainties in the fouling test results

The effect of tube wall temperature has not been studied in this test. The baseline curve in Figs. 5 and 7 was generated with data points at five velocities ranging from 0.6-2.4 m/s (1-10 Pa shear). The hot side inlet temperature for these tests varied between 330-350 °C. The one data point for the LF tube had a hot side inlet temperature of 340 °C. Tube wall temperatures were not measured, but if all the data for the baseline were at the temperature of 340 °C, the baseline curve would shift slightly up or down, and the

corresponding comparisons in Table 4 would be different.

Because of the higher heat transfer coefficient on the tube side of the LF structure compared to the plain tube, the tube wall temperature will be lower and could partially explain the fouling reduction.

The fouling resistance measurement uncertainty was mentioned previously as $\pm 3.0\%$. This uncertainty was calculated for one of the five points on the baseline curve of Fig. 5. If similar uncertainties are calculated for each data point and used to draw upper and lower bounds on both the baseline curve as well as the LF data point, a band of improvement can be estimated instead of the single values shown in Table 4.

Further work

Our data show that fouling reduction can be obtained with the LF structure. However, we have a single data point as evidence and a systematic study with flow variations would better quantify the effect. Field applications could be initiated using the numbers in Tables 3 and 4, with the understanding that the differences between the plain and LF tubes may not match the ratios shown here if the flow rates are substantially different.

Theoretical work regarding the distribution of shear stress on the fins, the effect of fins on the wall temperature, and the effect of wall temperature itself can help to further quantify the fouling improvement under different conditions.

CONCLUSIONS

1. Tube side heat transfer enhancement techniques can also be beneficial to mitigate fouling.
2. The Wieland tube with the LF inside structure provided a fouling reduction of 57% (100-43, referring to Table 4) based on tube external surface and a heat transfer increase of 21%, but with a pressure drop increase of 63%.
3. It may be possible to predict the amount of fouling reduction provided by an enhancement technique if a shear stress can be calculated.
4. The benefit of enhancement and fouling mitigation is at the expense of pressure drop (or pumping power), but could be economically justified, which can be proven with techniques such as PEC.

NOMENCLATURE

A	Tube outside surface area, πDL , m^2
C_p	Crude specific heat, $kJ/kg\cdot K$
D	Tube outside diameter, m
ID	Inside diameter, mm
L	Tube length, m
LMTD	Log mean temperature difference, °C
m	Crude mass flow rate, kg/s
OD	Outside diameter, mm
Q	Heat duty, kW
R_f	Fouling resistance, $m^2\cdot C/W$
T_c	Crude bulk temperature, °C

U Overall heat transfer coefficient based on tube external surface, W/m²-C

Subscript

0 clean condition
c clean
f fouled condition
i inlet
o outlet

REFERENCES

Joshi, H. M., Kukulka, D. J., Kummari, S., 2014, Heat Transfer Performance Evaluation Criteria Applied to a Textured Tube Surface for Crude Oil, *J. Enhanced Heat Transfer*, Vol. 21 (4-5), pp. 397-405.

Fetisoff, P. E., Watkinson, A. P., and Epstein, N., 1982, Comparison of two heat transfer fouling probes, Proc. 7th Intl. Heat Transfer Conf., eds. U. Grigull, E. Hahne, K. Stephan, and J. Straub, Hemisphere, Washington, DC, p. 391.

Hout, S.A. 1983. Chemical Reaction Fouling. Ph. D. Thesis, University of Bath, UK.

Harris, J., Lane, M., Smith, A., 2017, Investigating the Impact of Boiling Conditions on the Fouling of a Crude Oil, *Heat Transfer Engineering*, Vol. 38, Iss. 7-8, pp. 703-711

Webb, R. L., Li, W., 2000, Fouling in Enhanced Tubes Using Cooling Tower Water. Part I: Long-Term Fouling Data. *International Journal of Heat and Mass Transfer*, Vol. 43, pp. 3567-3578

Webb, R. L., Kim, N-H., 2005, *Principles of Enhanced Heat Transfer*, 2nd Ed., pp. 372-375, Publ. Taylor & Francis